Biochimica et Biophysica Acta 1788 (2009) 2114–2123

Contents lists available at ScienceDirect

Biochimica et Biophysica Acta

journal homepage: www.elsevier.com/locate/bbamem

Review

Cholesterol-induced fluid membrane domains: A compendium of lipid-raft ternary phase diagrams

Derek Marsh

Max-Planck-Institut für biophysikalische Chemie, Abteilung Spektroskopie und photochemische Kinetik, 37070 Göttingen, Germany

ARTICLE INFO

Article history:
Received 18 May 2009
Received in revised form 20 July 2009
Accepted 13 August 2009
Available online 21 August 2009

Keywords:
Membrane domains
Lateral phase separation
Lipid phase diagrams
Cholesterol
Lipid raft

ABSTRACT

The biophysical underpinning of the lipid-raft concept in cellular membranes is the liquid-ordered phase that is induced by moderately high concentrations of cholesterol. Although the crucial feature is the coexistence of phase-separated fluid domains, direct evidence for this in mixtures of cholesterol with a single lipid is extremely sparse. More extensive evidence comes from ternary mixtures of a high chain-melting lipid and a low chain-melting lipid with cholesterol, including those containing sphingomyelin that are taken to be a raft paradigm. There is, however, not complete agreement between the various phase diagrams and their interpretation. In this review, the different ternary phase diagrams of cholesterol-containing systems are presented in a uniform way, using simple *x,y*-coordinates to increase accessibility for the non-specialist. It is then possible to appreciate the common features and examine critically the discrepancies and hence what direct biophysical evidence there is that supports the raft concept.

Contents

1. Introduction

Of the ca. 260 lipids constituting the yeast lipidome, ergosterol is the most abundant [1]. This is likely to be true also for cholesterol in higher organisms, where it is present in the plasma membranes at a roughly equimolar ratio with respect to total phospholipid. The function of cholesterol in membranes is partly as a fluidity regulator, condensing the chains of unsaturated lipids in fluid L_α phases and fluidizing those of saturated lipids that would otherwise form solid-like L_β gel phases [2,3].

The idea that cholesterol may play an additional functional role in membranes came with the theoretical suggestion, following earlier experiment-based proposals of partial binary phase diagrams [4], that cholesterol could induce a separate phase – the liquid-ordered phase (L_o) – that is distinct from the solid-ordered L_β gel phase and the liquid-disordered L_α fluid phase [5]. Definitive experimental evidence for the existence of such a separate phase was provided first by two-component ^{2}H NMR spectra from the perdeuterated chains of gel-phase (not fluid-phase) lipids in the presence of cholesterol [6,7]. Possible implications of this novel phase in cell biology came from the proposal of lipid rafts as functional platforms involved both in the compartmentation of cellular membranes and in the directing of intracellular membrane traffic [8].

The original raft concept was based on compositional differences, in both lipids and proteins, that are found between the apical and basolateral membranes in polarized epithelial cells, and the specific targeting of membrane components that this implies. The apical membrane is characterized particularly by a high content of sphingolipids (which have intrinsically high chain-melting temperatures [9]) and of cholesterol. This is a lipid composition that favours formation of L_o phases. On the other hand, the usual glycerolipids of the basolateral membrane bear unsaturated *sn*-2 chains that favour formation of L_α phases. Both

E-mail address: dmarsh@gwdg.de.

0005-2736/$ – see front matter © 2009 Elsevier B.V. All rights reserved.
doi:10.1016/j.bbamem.2009.08.004

L_α and L_o are fluid phases and, therefore, can form domains that support functional incorporated membrane enzymes and transport systems (see, e.g., [10]). Thus, the biophysical correlate of membrane raft formation is the fluid–fluid phase separation between L_α and L_o lipid domains.

Observation of lipid rafts in biological membranes has proved rather elusive, and consequently, direct detection of L_α–L_o phase separation in model membranes of defined composition is an important aspect of the raft concept. Although not entirely absent, direct evidence for fluid–fluid phase separation in binary mixtures of a single phospholipid and cholesterol is also extremely sparse. Historically, indirect evidence for fluid–fluid immiscibility in a phospholipid–cholesterol mixture was provided first by spin-labelled lipids [4], which also led to the original suggestion that coexistence of immiscible phases in cell membranes would be of biological significance and to the discovery of liquid–liquid immiscibility in phosphatidylcholine–cholesterol monolayers [11] that is now seen also in asymmetric bilayers [12]. Most direct evidence for L_α–L_o phase separation in bilayers comes currently, however, from ternary mixtures of cholesterol with two lipids that have, respectively, a low and a high chain-melting temperature. Ternary phase diagrams of such cholesterol-containing lipid mixtures are, therefore, of central interest but are not without controversial aspects.

Here, I collect together all the available phase diagrams of the above type. This encompasses those with sphingomyelin or a fully saturated phosphatidylcholine as the high-melting lipid and an unsaturated or short-chain phosphatidylcholine as the low-melting lipid. To increase accessibility to a wider readership, I give the experimental ternary phase diagrams in simple *x*–*y* coordinates, instead of the triangular, 60°-inclined coordinates that are used almost exclusively in the literature for presenting the original data. This compact *x*–*y* representation considerably simplifies intercomparison of the different data sets, making it possible to appreciate the common features and examine critically the discrepancies. First, I summarise the salient features of the triangular representation, before going on to explain the relationship with the simple *x*,*y* representation. Then, I use the latter to present all the available ternary phase diagrams and hence to highlight what hard data currently support the membrane raft hypothesis.

A reviewer of this paper remarked that every paper in this field should define its use of the term "raft." For the purpose of this review, the restricted position taken here is that without coexistence of L_α and L_o domains – of whatever size – lipid rafts do not exist.

2. Ternary phase diagrams

In the triangular representation, the compositions of ternary mixtures in mole fractions are given by the set of points contained within an equilateral triangle of unit side, as indicated in Fig. 1. For any composition, P, the mole fractions (X_A, X_B, X_C) of lipids A, B, and C (cholesterol) are given by the triangular coordinates of P along the directions CA, AB, and BC, respectively. From the geometry of an equilateral triangle, the sum of the three coordinates is equal to the length of a side, which ensures that: $X_A + X_B + X_C = 1$, as is required for mole fraction units. A straight line from the cholesterol vertex C of the triangle (generically referred to as a "diagonal") represents compositions with a fixed mole ratio of the lipid components A and B, which is determined by the intercept (X_o) on the opposite side (AB). Thus, for any composition P on the line CX_o, the mole ratio of lipid B to lipid A is $X_B / X_A = X_o / (1 - X_o)$. Equivalent relations hold for "diagonals" from the two other vertices.

More generally, if a system of composition α is mixed in any proportion with one of composition β, the total composition of the mixture P will lie on a straight line (a tie line) that joins α and β (see a particular case in Fig. 1). The fraction of α in the mixture is given by the lever rule:

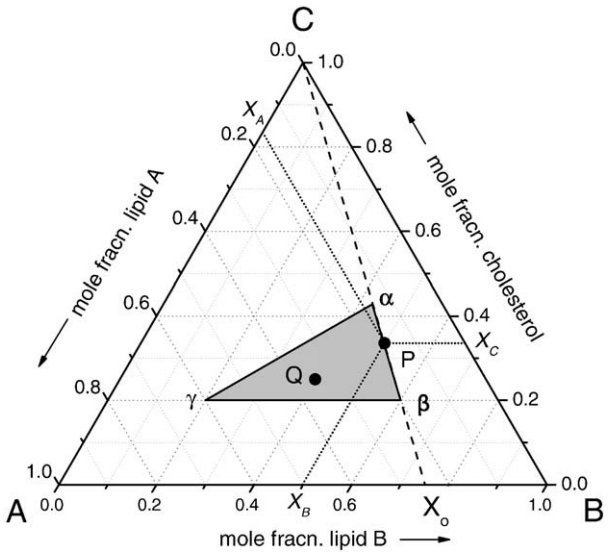

Fig. 1. Triangular representation of the compositions of ternary mixtures of lipids A and B with cholesterol (C). The axes to which mole fraction coordinates (X_A, X_B, X_C) are referred are tilted at 60° to one another. α–β, β–γ and α–γ are tie lines and αβγ is a three-phase triangle.

$$f = \frac{X_{B,\beta} - X_B}{X_{B,\beta} - X_{B,\alpha}} \tag{1}$$

where $X_{B,\alpha}$ and $X_{B,\beta}$ are the mole fractions of B in the systems α and β, respectively. Equivalent expressions hold with the mole fractions of components A and C. Analogously, the total composition Q of a system in a three-phase region lies within the triangle αβγ that is bordered by intersecting tie lines for the constituent two-phase systems αβ, βγ, and αγ.

3. Phospholipid–cholesterol ternary phase diagrams in *x*,*y*-coordinates

The phase diagrams of hydrated lipid ternary mixtures with cholesterol are routinely presented in the literature as triangular *x*,*y*,*z*-coordinates in the so-called Gibbs triangle, as indicated above. Because cholesterol does not itself form bilayer membranes and can be incorporated into lipid bilayers at maximally a 2:1 mole ratio (much less for certain unsaturated lipids [13–15]), there is no overriding advantage to using 60°-inclined axes rather than the familiar orthogonal *x*,*y*-axes. Fig. 2 shows two representations of the ternary phase diagram for 1-palmitoyl-2-oleoyl phosphatidylcholine (POPC)/*N*-palmitoyl sphingomyelin (PSM)/cholesterol mixtures from de Almeida et al. [16]. On the left, the *x*-axis is the mole fraction of PSM relative to total phospholipid, $x = \mathrm{PSM}/(\mathrm{PSM} + \mathrm{POPC})$, as in a binary phase diagram; and the *y*-axis is the cholesterol to total phospholipid mole ratio, $y = \mathrm{cholesterol}/(\mathrm{PSM} + \mathrm{POPC})$, that is often used for discussing binary mixtures of lipids with cholesterol. From the conservation of mass, the mole ratio of cholesterol to phospholipid, *y*, in a region of coexisting phases α and β is given by:

$$y = f y_\alpha + (1 - f) y_\beta \tag{2}$$

where *f* is the fraction of the α phase, and y_α and y_β are the mole ratios of cholesterol to phospholipid in phases α and β at the

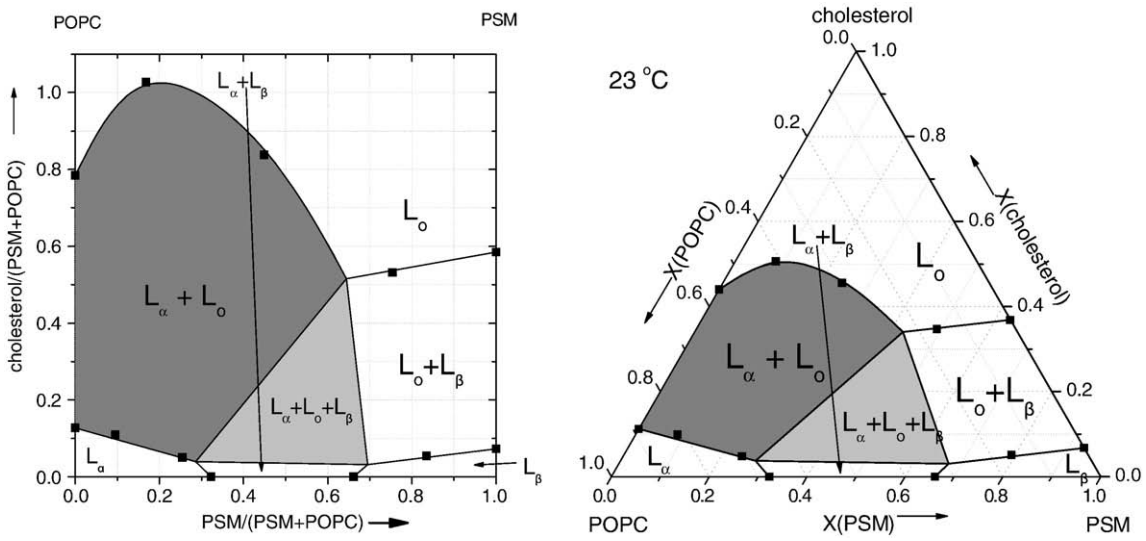

Fig. 2. Phase diagram for ternary mixtures of 1-palmitoyl-2-oleoyl phosphatidylcholine (POPC), *N*-palmitoyl sphingomyelin (PSM) and cholesterol at 23 °C. *Right*: triangular (60°-inclined) coordinates; all compositions are given as mole fraction with respect to total phospholipid plus cholesterol. *Left*: rectilinear coordinates; the abscissa is the mole fraction of PSM solely with respect to phospholipid (i.e., PSM + POPC) and the ordinate is the mole ratio of cholesterol to total phospholipid (PSM + POPC). The region of two coexisting fluid phases is shaded grey and that of three-phase coexistence is shaded light grey. Data from De Almeida et al. [16].

respective ends of the tie line. A similar relation holds for the mole fraction, *x*, of PSM in the phospholipid mixture:

$$x = fx_\alpha + (1-f)x_\beta \tag{3}$$

where x_α and x_β are the phospholipid mole fractions of PSM in phases α and β at the respective ends of the tie line. Thus the two are linearly related, and therefore, tie lines are straight, the three-phase triangle is preserved, and fixed cholesterol/PSM or POPC ratios lie on diagonals in this simple *x*–*y* representation and in a way more transparent than in the triangular representation (cf., Fig. 1).

For comparison, the triangular representation of the same phase diagram is given on the right of Fig. 2, with compositions expressed as mole fractions relative to the total ternary mixture, e.g., *X*(cholesterol) = cholesterol / (cholesterol + PSM + POPC). Relative to total mole fraction units, the cholesterol to phospholipid mole ratio is elongated at higher cholesterol contents. This effect is only excessive at compositions outside the region of interest. The advantages of using cholesterol/lipid mole ratio, instead of mole fraction, in the left-hand diagram are the linear dependences that were described above (Eqs. (2) and(3)). As already mentioned, cholesterol mole ratio is frequently used in discussing cholesterol–phospholipid interactions and is also the quantity that determines cholesterol solubility in lipid bilayer membranes. Here, I shall present all published ternary phase diagrams in mixtures with cholesterol by using the simple *x*,*y*-coordinates. This also has the advantage of compactness, which eases comparison between the different data on the same system.

4. Phosphatidylcholine/sphingomyelin/cholesterol mixtures

Historically, Fig. 2 (right) from de Almeida et al. [16] was the first phase diagram to be published for a ternary lipid mixture with sphingomyelin and cholesterol. Because the high-melting lipid component is a sphingolipid and the low-melting lipid component is an *sn*-2 unsaturated phosphatidylcholine, it corresponds most closely to a natural membrane lipid composition and has come to be considered as the canonical raft–lipid mixture. Phase coexistence was not detected directly in constructing the phase diagram in Fig. 2; instead, phase boundaries were detected from the spectroscopic properties of fluorescent lipid probes, *trans*-parinaric acid and diphenyl hexatriene.

Figs. 3 to 5 collect together all further published ternary phase diagrams for mixtures of sphingomyelin (SM) and a low-melting phosphatidylcholine (PC) with cholesterol. Figs. 3 and 5 are based on

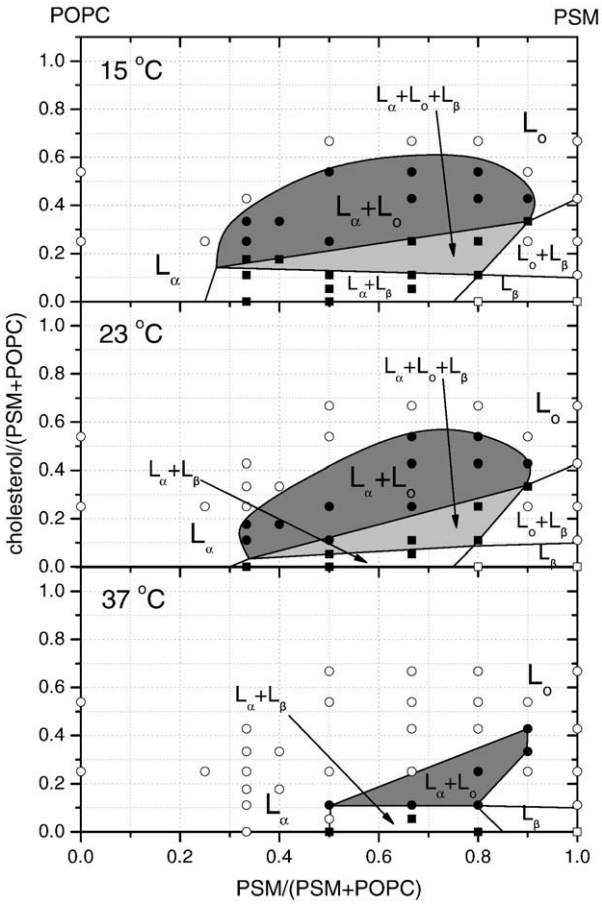

Fig. 3. Ternary mixtures of POPC, PSM, and cholesterol at the temperatures indicated. Open circles correspond to a single fluid phase, solid circles to coexisting fluid phases, open squares to the absence of gel phase, and solid squares to the presence of gel phase. Data from Veatch and Keller [17]. Phase boundaries are drawn in analogy to those for 15 °C in the original publication.

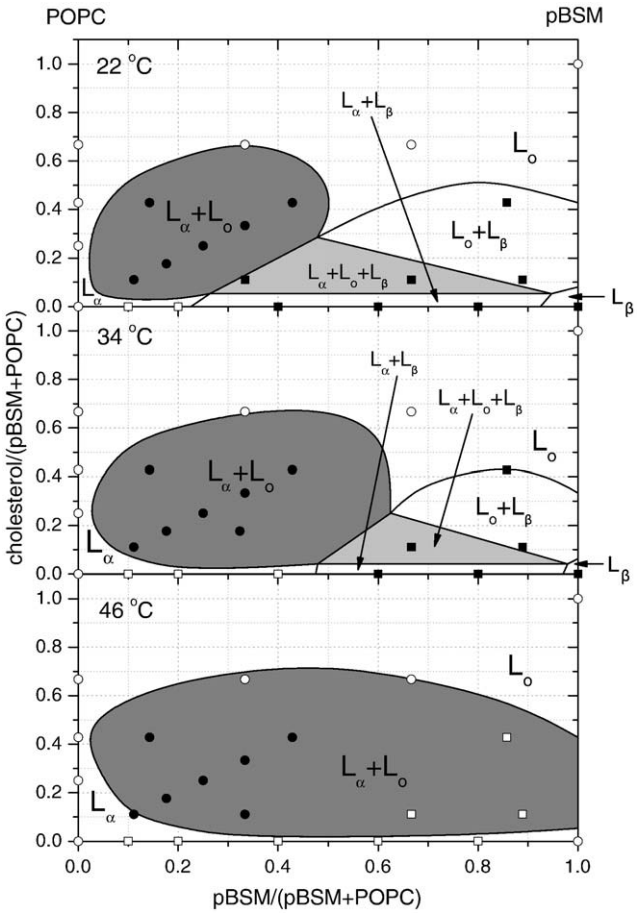

Fig. 4. Ternary mixtures of POPC, porcine brain sphingomyelin (pBSM), and cholesterol at the temperatures indicated. Open circles correspond to a single fluid phase, solid circles to coexisting fluid phases, open squares to the absence of gel phase, and solid squares to the presence of gel phase. Data from Pokorny et al. [18].

observation of domains in giant unilamellar vesicles (GUVs) under the fluorescence microscope [17]. Fig. 4 is for porcine brain SM (pBSM) which contains predominantly C(18:0) (49%) and C(24:1) (20%) *N*-acyl chains, in contrast to C(16:0) for PSM. In this case, the region of fluid-phase (L_α–L_o) coexistence is mapped out by studying the kinetics of trapped dye release from large unilamellar vesicles (LUVs), which is induced by the peptide δ-lysin, and the presence of gel phase is detected calorimetrically [18]. Gel–fluid coexistence causes ion leak arising from mismatch at the phase boundaries [19], but the mismatch at fluid–fluid boundaries is less pronounced, more difficult to detect, and therefore requires enhancement by preferential targeting of membrane-active peptides. In fact, the original authors propose that the principal effect of L_α–L_o phase coexistence on dye release arises from concentration of δ-lysin in L_α domains, because it is excluded from L_o domains [18].

All phase diagrams for SM-containing systems (Figs. 2–5) share the common features of a three-phase triangle ($L_\alpha + L_o + L_\beta$) and a region of fluid–fluid ($L_\alpha + L_o$) coexistence, in addition to two regions of gel–fluid coexistence ($L_\alpha + L_\beta$ and $L_o + L_\beta$) that extend to the axes for the binary mixtures. It should be noted, however, that in none of the cases has the coexistence of three phases been demonstrated directly: the three-phase triangle is inferred indirectly on thermodynamic grounds. Although some differences between the various phase diagrams in Figs. 2–5 can be attributed to the different lipids used, pBSM vs. PSM and dioleoyl PC (DOPC) vs. POPC, there remain considerable differences in location of the various phase boundaries, especially for Figs. 2 (left) and 3 (middle) that refer to exactly the same lipids and temperature. These discrepancies must be attributed to the different experimental methods that are used to determine the phase boundaries, in addition to uncertainties in inference of the three-phase region.

The most significant qualitative difference between Figs. 2 and 3 is that the region of raft ($L_\alpha + L_o$) coexistence extends out to the binary mixture POPC + cholesterol, which lies along the $x = 0$ axis in Fig. 2. This is a controversial area. Currently, evidence for L_α–L_o coexistence in this binary mixture at 23 °C and above is indirect. It rests upon theoretically expected linear dependences for the fluorescence polarization of diphenyl hexatriene and the mean fluorescence lifetime of *trans*-parinaric acid on mole fraction of cholesterol in a two-phase region [16] and also on the fluorescence polarization and biphasic distribution of fluorescence lifetimes for *trans*-parinaric acid [20]. The absence of fluid–fluid coexistence for POPC + cholesterol in Fig. 3 could be because the domains are too small to be detected by light microscopy (less than ~300 nm). This is certainly the case for gel–fluid (L_β–L_o) coexistence in binary mixtures with cholesterol (see open circles indicating uniform fluorescence along the entire $x = 1$ axis in Figs. 3 and 5), where there is clear evidence for phase coexistence in PSM–cholesterol mixtures from two-component lipid spin-label EPR spectra [21]. Note that the boundaries of the L_β–L_o coexistence regions in Figs. 3 and 5 are simply inferred and not located from fluorescence microscopy.

^{2}H NMR spectroscopy yields two-component spectra in the gel regime of binary POPC–cholesterol mixtures, indicating L_β–L_o phase coexistence [7]. But it does not yield two-component spectra in the putative L_α–L_o coexistence region: only a broadening of the single-

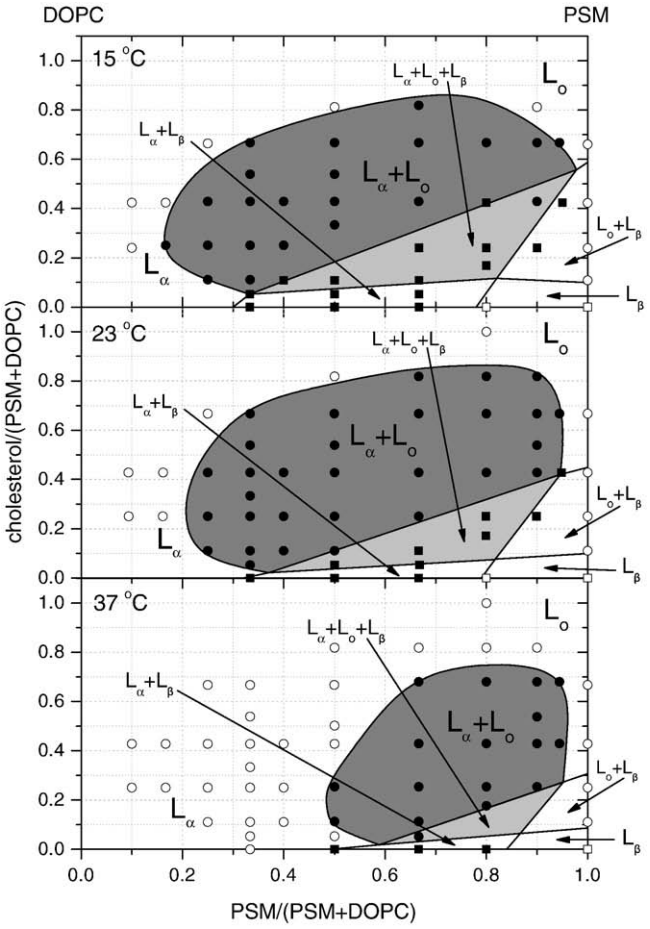

Fig. 5. Ternary mixtures of dioleoyl phosphatidylcholine (DOPC), PSM, and cholesterol at the temperatures indicated. Open circles correspond to a single fluid phase, solid circles to coexisting fluid phases, open squares to the absence of gel phase, and solid squares to the presence of gel phase. Data from Veatch and Keller [17]. Phase boundaries are drawn in analogy to those in Fig. 3.

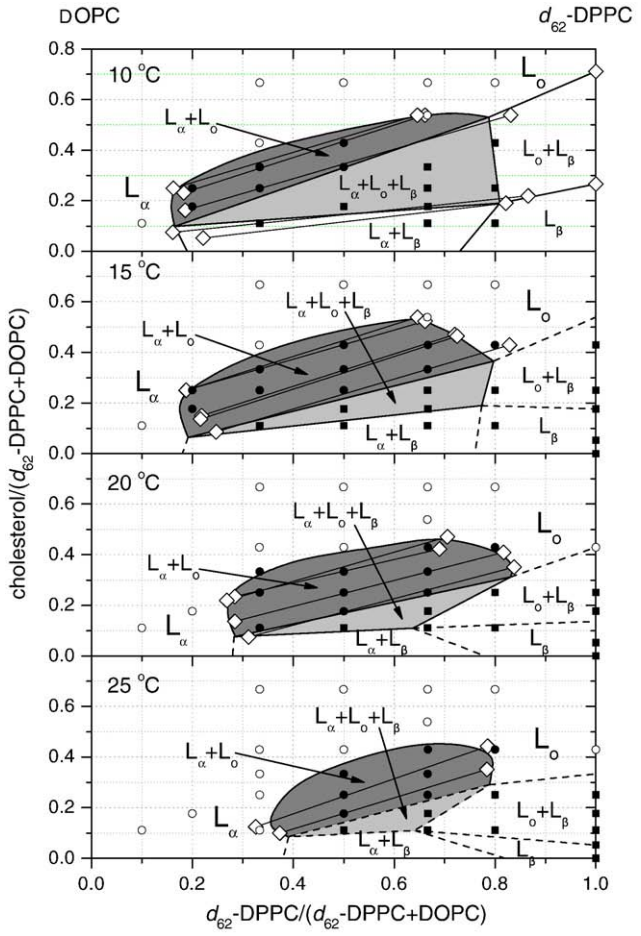

Fig. 6. Ternary mixtures of DOPC, chain-perdeuterated dipalmitoyl phosphatidylcholine (d_{62}-DPPC) and cholesterol at the temperatures indicated. Open circles correspond to a single fluid phase [also for cholesterol / (DPPC + DOPC) = 1.0], solid circles to coexisting fluid phases, and solid squares to the presence of gel phase. Lines connecting diamonds are tie lines in the various two-phase regions. Data from Veatch et al. [29].

component spectra, which might arise from exchange between small domains. However, ^{2}H NMR does reveal a horizontal phase boundary with the L_β–L_o coexistence region at ca. −7 °C (for *sn*-1 chain-perdeuterated POPC), which implies L_α–L_o coexistence at temperatures immediately above this boundary [7]. Thus, the only real uncertainties for the POPC + cholesterol system are the size of the domains and the location of the miscibility transition temperature at which fluid–fluid phase separation disappears.

Interestingly, there seems to be a consensus that fluid-phase immiscibility does not occur in mixtures of DOPC and cholesterol [22–25] (cf., Fig. 5), although this binary system has been investigated neither by ^{2}H NMR in the gel temperature regime nor by *trans*-parinaric acid and diphenyl hexatriene fluorescence in the fluid regime.

In addition to the qualitative differences, there are also quantitative differences between Figs. 2–4 with regard to the positioning and extent of the crucial "raft" L_α–L_o coexistence region. Whereas it is a major insight of Fig. 4 to detect L_α–L_o fluid–fluid phase separation by means of peptide-enhanced ion permeability, the kinetics of leakage may not have the sensitivity to establish actual phase boundaries precisely. Perhaps the same might also be said about the detection of L_α–L_o phase coexistence from analysis of *trans*-parinaric acid fluorescence lifetimes. At first glance, direct visualization of coexisting lipid domains by fluorescence microscopy (Figs. 3 and 5) provides the ideal answer.

Unfortunately, it has been found that micron-sized domains can be produced by photochemically-induced processes under the influence of illumination [26,27]. Formation of light-induced domains is promoted by high concentrations of fluorescent probe, high levels of illumination, long duration of illumination, the presence of unsaturated lipids (including SM), electrolytic processes accompanying the electroformation used in producing GUVs for microscopy, and crucially the presence of oxygen. The kinetics of light-induced domain formation depend on the lipid composition, viz., on the cholesterol content [27]. Whereas the latter might suggest that detection of domains produced by illumination indicates the presence of pre-existing submicroscopic domains, it cannot be excluded on the other hand that "instantaneous" domains are light-induced with rapid kinetics. The closer to a phase boundary detected by fluorescence microscopy, the faster is the production of light-induced domains [27]. Under these circumstances, there is uncertainty associated with the exact position of the phase boundaries, if the influence of factors affecting formation of irradiation-induced domains is not investigated, particularly the exclusion of oxygen and addition of antioxidants.

One solution to these potential uncertainties comes from ^{2}H NMR, which has been used to study ternary mixtures of phosphatidylcholines with cholesterol.

5. Low-melting PC/high-melting PC/cholesterol

Although fully saturated phospholipids occur only rarely in most biological membranes, those with higher chain-melting temperatures can act as a surrogate for the sphingolipid component in ternary mixtures representing model lipid rafts. Results on mixtures of a high-melting PC with a low-melting PC and cholesterol are more numerous than for the SM counterpart. The ternary phase diagrams of these systems are presented in Figs. 6 to 10. In these figures and what

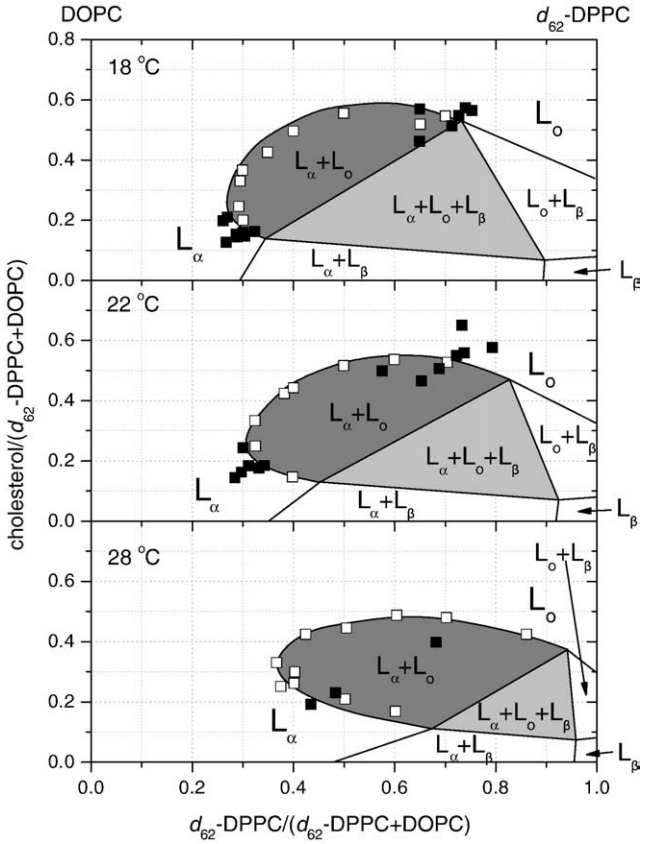

Fig. 7. Ternary mixtures of DOPC, d_{62}-DPPC, and cholesterol at the temperatures indicated. Solid squares correspond to approximate ends of tie lines; open squares are boundaries interpolated from temperature dependences. Data from Davis et al. [38].

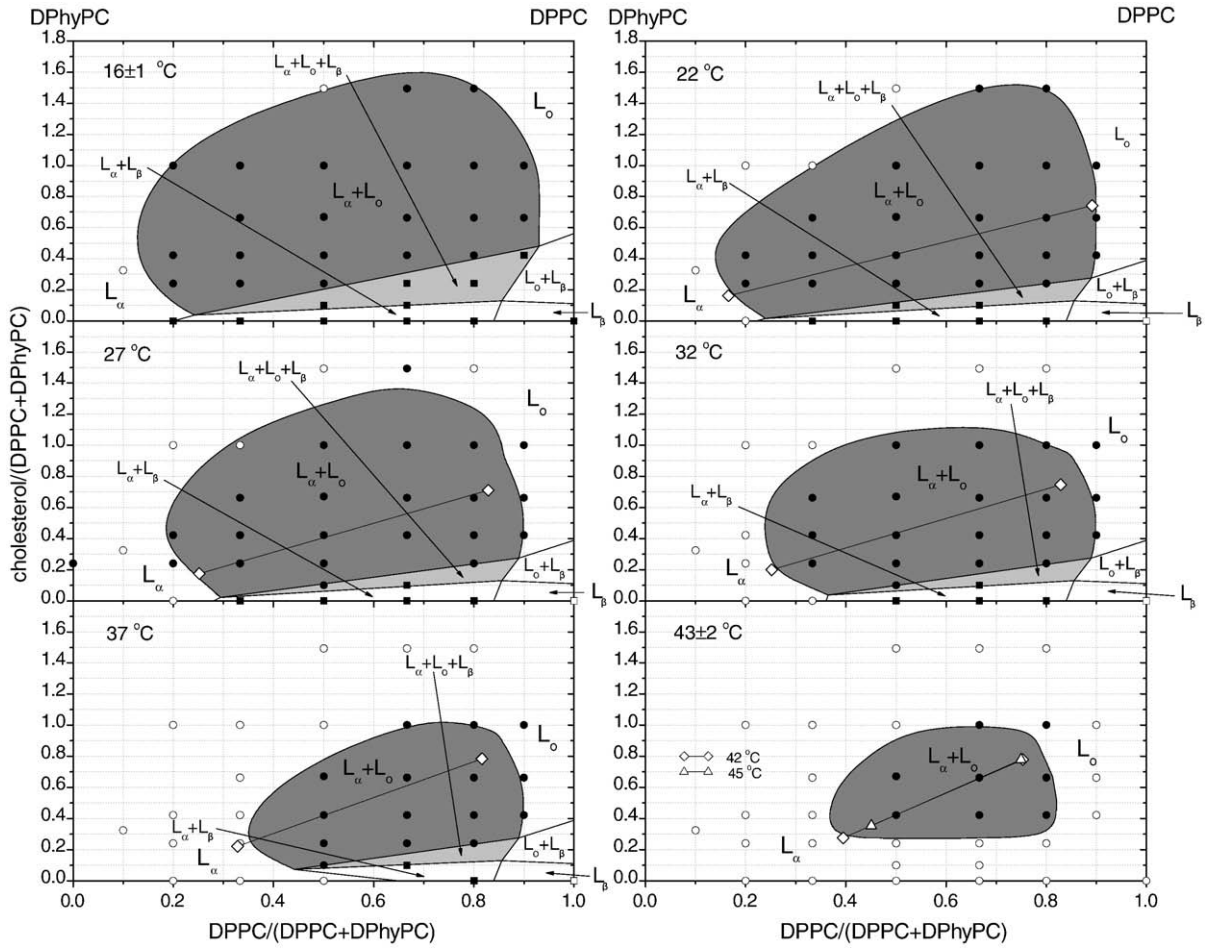

Fig. 8. Ternary mixtures of diphytanoyl phosphatidylcholine (DPhyPC), DPPC and cholesterol at the temperatures indicated. Open circles correspond to a single fluid phase, solid circles to coexisting fluid phases, open squares to the absence of gel phase, and solid squares to the presence of gel phase. Lines connecting diamonds (and triangles) are tie lines in the various two-phase regions. Data from Veatch et al. [39]. Phase boundaries are drawn in analogy to those for 16 °C and 43 °C in the original publication.

follows, L_β is used generically to designate PC gel phases. Details of gel-phase coexistences involving the $P_{\beta'}$ and $L_{\beta'}$ phases are not taken into account. It should be noted that both the chain tilt in the $L_{\beta'}$ phase and the pretransition between $L_{\beta'}$ and $P_{\beta'}$ phases of saturated PCs are eliminated at relatively low cholesterol contents [28].

Dipalmitoyl PC (DPPC) replaces SM as the high-melting lipid in Fig. 6 and DOPC is the low-melting partner. This phase diagram is determined solely from ^{2}H NMR by using DPPC with perdeuterated chains and is notable for the considerable numbers of tie lines, which are located by identifying spectra that contain the same two components differing only in their relative proportions [29]. The slopes of these tie lines, which largely determine the orientation of the three-phase region, can be expressed intuitively in the *x*,*y* representation and are listed in Table A.1 of the Appendix.

That well resolved two-component ^{2}H NMR spectra are observed in the raft coexistence region containing L_α and L_o domains in this three-component system is noteworthy. It implies that the domains are too large for spectral averaging to occur by translational diffusion of lipids between these different fluid domains. The two-dimensional equivalent of the Einstein equation for Brownian diffusion gives the mean-square distance traveled in time t' as:

$$\langle r^2 \rangle = 4D_T t' \tag{4}$$

where D_T is the translational diffusion coefficient. Typical lipid lateral diffusion coefficients are $D_T \sim 10\ \mu m^2\ s^{-1}$ in L_α phases and a factor of two lower in L_o phases [22,30]. That the smallest quadrupole splittings (those of the chain terminal methyls, for which the difference is: $\delta\Delta\omega_Q \sim 6\times10^3$ rad s^{-1}) not be averaged by translational diffusion requires domain diameters considerably in excess of 0.1–0.2 μm (see, e.g., [31]). The coexisting L_α and L_o domains that are visualized by fluorescence microscopy are much larger than this lower limit [32,33], although estimates of domain sizes from fluorescence energy transfer for POPC/SM/cholesterol mixtures include some values within this range [34,35]. For EPR of spin-labelled lipids, by comparison, the smallest differences in splittings between L_o- and L_α-phase spectra (for the 14- or 16-positions of the chains) are approximately 10^4 times greater than in ^{2}H NMR [21] and therefore require domain diameters 100 times smaller, i.e., these should be considerably greater than ~1 −2 nm to avoid averaging by translational diffusion. This suggests that, in addition to detecting domain coexistence, two-component EPR spectra might also detect transient cluster formation arising from critical fluctuations, but only if these are slower than the characteristic 10−100 MHz frequency range of the spin-label EPR splittings. Current ^{2}H NMR analysis of critical fluctuations concentrates on frequencies in the range of 0.1−10 MHz [29,36]. For phase coexistence, on the other hand, the individual components of two-component spectra should be identical to the single-component spectra from the immediately adjacent single phases. Broadening may occur from exchange between domains, if these are sufficiently small, or alternatively from fluctuations if the system is close to a critical point. In general, phase coexistence and formation of clusters from critical behaviour can only be distinguished by a critical evaluation of the entire phase diagram and its dependence on temperature. A list of available data on

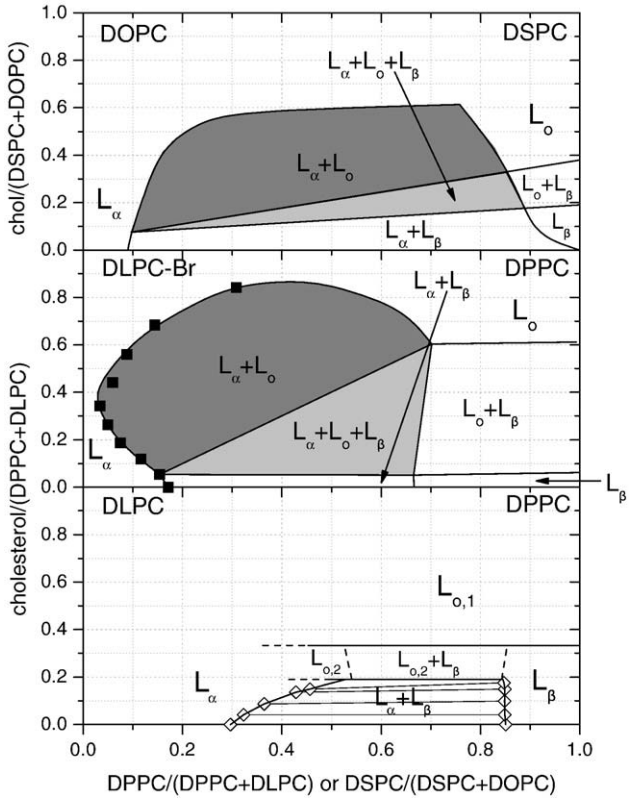

Fig. 9. Ternary mixtures (*top*) DOPC and distearoyl phosphatidylcholine (DSPC) or (*middle* and *bottom*) dilauroyl phosphatidylcholine (DLPC) and DPPC, with cholesterol. In the middle panel, DLPC bears a single Br on C-12 of the *sn*-2 chain. In the bottom panel, the region designated $L_{o,2}+L_\beta$ may be a continuous transition; lines joining diamonds are tie lines. Temperatures: 23 °C, 25 °C, and 24 °C for top, middle, and bottom, respectively. Data from *top*: Zhao et al. [45], *middle*: Silvius et al. [43], and bottom: Feigenson and Buboltz [46] and Chiang et al. [44].

miscibility critical temperatures is included in the Appendix (Table A.4).

As already noted for POPC + cholesterol, the situation is different for L_α–L_o coexistence in binary mixtures, including DPPC + cholesterol [6], 1-palmitoyl-2-petroselinoyl PC + cholesterol [7] and 1-stearoyl-2-elaidoyl PC (SEPC) + cholesterol [37]. Two-component ^{2}H NMR spectra were not observed in the putative $L_\alpha + L_o$ regime for any of these binary systems (but see [38]), although two-component spectra that correspond to L_β–L_o phase coexistence in the gel-phase regime are seen clearly. Indeed, as stated in the Introduction, ^{2}H NMR spectroscopy of DPPC + cholesterol binary mixtures provided the first, and unambiguous, experimental identification of the liquid-ordered phase in lipid bilayer membranes, but only in coexistence with the gel phase [6]. For two-component ^{2}H NMR spectra not to be detected in the $L_\alpha + L_o$ region, the largest quadrupole splittings (those of the order-parameter plateau region for which: $\delta\Delta\omega_Q \sim 7\times10^4$ rad s^{-1}) must be averaged by translational diffusion. This requires diameters of considerably less than 30–50 nm for the phase-separated domains, which is consistent with them not being visualized by fluorescence microscopy (cf., [32,33]).

A notable feature of the phase diagrams in Fig. 6 is that the three-phase regions are identified from composite ^{2}H NMR spectra, which consist of the same three components in different proportions. This is the first case in which coexistence of three phases has been demonstrated directly for several compositions. Three coexisting phases had been visualized shortly before by fluorescence lifetime imaging of a GUV with overall composition DOPC/DPPC 1:1 mol/mol + 12 mol% cholesterol at 24 °C [23]. This point ($x=0.5$, $y=0.136$) is located within the three-phase triangles at 20 and 25 °C for the equivalent ternary mixture with d_{62}-DPPC in Fig. 6 (and in the phase diagram for 22 °C in Fig. 7).

Fig. 7 presents phase diagrams also for the DOPC/DPPC/cholesterol system, also determined from ^{2}H NMR spectroscopy. Although there are overall similarities to Fig. 6 in the location of the L_α–L_o coexistence region and orientation of the tie lines at comparable temperatures, there are appreciable differences, and even greater differences in the L_o–L_β coexistence region and in the three-phase triangle. The $L_o + L_\beta$ phase boundaries in Fig. 7 are determined at $x=1$ by the data of Vist and Davis [6] for DPPC + cholesterol binary mixtures, whereas those in Fig. 6 are based on the tie line established for $x=1$ at 10 °C (upper panel). Although three-component spectra were identified, this was insufficient to position the boundaries of the three-phase region in Fig. 7 [38]. The border of the three-phase triangle with the $L_\alpha + L_o$ region was located from the extent of this two-phase region, but the vertex involving coexistence with the L_β gel phase could not be determined accurately.

DPPC is again the high-melting lipid in Fig. 8, but the low-melting lipid is diphytanoyl PC. Phytanic acid has an extensively methyl-branched chain (3,7,11,15-Me$_4$-16:0), the ether-linked version of which in archaeal membrane lipids is a chemically more stable alternative to the *cis*-unsaturated chains found in bacteria and higher organisms. This ternary, cholesterol-containing system gives rise to a particularly large range of $L_\alpha + L_o$ domain coexistence, as detected by fluorescence microscopy. Fluid–fluid phase separation is observed by two-component ^{2}H NMR spectra from DPPC with perdeuterated chains, and estimated end points for tie lines through the composition DPhyPC/DPPC 1:1 + 30 mol% cholesterol ($x=0.5$, $y=0.43$) lie reasonably close

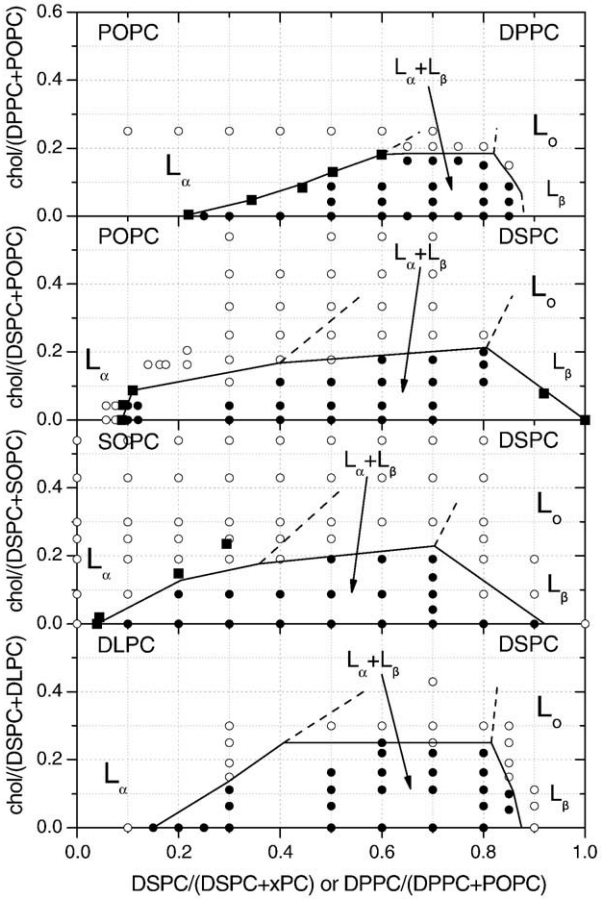

Fig. 10. Ternary mixtures of (*top* to *bottom*): POPC–cholesterol–DPPC, POPC–cholesterol–DSPC, 1-stearoyl-2-oleoyl phosphatidylcholine (SOPC)–cholesterol–DSPC, and DLPC–cholesterol–DSPC, at 23 °C. Solid circles represent two coexisting phases, open circles represent vesicles showing uniform fluorescence, and solid squares are phase boundaries. Data from Zhao et al. [27].

(but are not identical) to the phase boundaries constructed from fluorescence microscopy (see Fig. 8). The observation of immiscibility at temperatures above that for chain-melting of DPPC has led to the proposal of a phase diagram with two miscibility critical points (see 43 °C in Fig. 8). With the direction of the tie lines determined by ^{2}H NMR, this would virtually exclude $L_\alpha + L_o$ phase separation for binary mixtures of DPPC + cholesterol, because the tie line would end at the boundary of a two-phase region [39]. Although most of the evidence for $L_\alpha + L_o$ phase coexistence in the binary system DPPC + cholesterol was indirect at the time, this was still a controversial suggestion because the upper boundary of $L_\beta + L_o$ coexistence region is practically horizontal in the binary phase diagram [6,40]. More recently, two-component ^{2}H NMR spectra have been observed for DPPC + 25 mol% cholesterol at temperatures immediately above that for chain-melting of DPPC with perdeuterated chains [38]. Even prior to this, $L_\alpha + L_o$ phase coexistence had been demonstrated for binary mixtures of PSM and cholesterol at a temperature well above the chain-melting transition of PSM, from two-component EPR spectra of spin-labelled phospholipids [21]. Therefore, present evidence indicates $L_\alpha + L_o$ phase coexistence in DPPC + cholesterol binary mixtures, at least at temperatures immediately above the horizontal phase boundary, but this is not detected by fluorescence microscopy presumably because the domains are too small.

Fig. 9 (top and bottom panels) compares two phase diagrams, for DOPC/distearoyl PC (DSPC)/cholesterol and dilauroyl PC (DLPC)/DPPC/cholesterol, both from the same laboratory and both deduced by using fluorescence microscopy of GUVs. That with the greater difference in chain-melting temperature between the PC components (viz., DOPC and DSPC) corresponds to the general pattern presented in Figs. 2 to 8. In contrast, raft-like fluid–fluid phase coexistence is not observed for the DLPC/DPPC/cholesterol system, only phase separation between gel and fluid phases. The latter is also the case for a series of PC–cholesterol ternary mixtures in which the difference in chain-melting temperature is less than that for DOPC and DSPC (see Fig. 10). For POPC/DPPC/cholesterol, POPC/DSPC/cholesterol, stearoyl-oleoyl PC (SOPC)/DSPC/cholesterol and DLPC/DSPC/cholesterol, the only domain formation detected is that corresponding to $L_\alpha + L_\beta$ phase separation, although these are systems for which light-induced domains are produced outside the $L_\alpha + L_\beta$ region [27]. This distinctly different pattern of observation in the fluorescence microscope was originally taken to indicate two quite different types of miscibility behaviour [41], but more recently, this view has been moderated [42]. The non-observation of $L_\alpha + L_o$ phase coexistence is now attributed to the small size of the domains. This interpretation is not surprising in view of the fact that $L_\beta + L_o$ phase coexistence cannot be visualized in DPPC–cholesterol binary mixtures by fluorescence microscopy [32], despite definitive evidence that it exists from ^{2}H NMR [6]. As is seen here, this region of gel–fluid phase separation is conspicuously missing from the phase diagrams shown in Fig. 10 and in the bottom panel of Fig. 9. Evidence for fluid–fluid phase separation in at least one of these systems comes from spectroscopy. The middle panel in Fig. 9 depicts the boundary of $L_\alpha + L_o$ phase coexistence for DLPC/DPPC/cholesterol that is determined from fluorescence quenching by a terminal bromine atom on the *sn*-2 chain of DLPC [43]. From this prescient early work, a phase diagram with extensive L_α–L_o coexistence is predicted that contains additionally all the features determined later by fluorescence microscopy, ^{2}H NMR and other techniques (cf., Figs 3–8).

6. Conclusions

Direct evidence for fluid–fluid phase separation of the $L_\alpha + L_o$ type in ternary phase diagrams of cholesterol-containing mixtures is less extensive than might generally be assumed. It would require an over-enthusiastic application of Occam's razor to discount all domains visualized by fluorescence microscopy as being light-induced, but if this were done, there remain only the phase diagrams supported by ^{2}H NMR for the two systems, DOPC/DPPC/cholesterol and DPhyPC/DPPC/cholesterol, that are given in Figs. 6–8. To these can be added three further ternary phase diagrams for POPC/PSM/cholesterol (Fig. 3), DOPC/PSM/cholesterol (Fig. 5), and DOPC/DSPC/cholesterol (Fig. 9), where coexisting $L_\alpha + L_o$ domains are visualized by fluorescence microscopy.

Putting aside statistical issues with GUVs, the great advantage of fluorescence microscopy is the demonstration of domains coexisting within the same membrane. Bulk measurements do not distinguish this from an inhomogeneous population of membranes. Potentially, inhomogeneities could arise from differential lipid solubilities in the organic solvent that is used to prepare the mixtures. Freeze–drying from a volatile organic solvent (and/or freeze–thaw) is not invariably applied, but for PC–cholesterol or SM–cholesterol mixtures, this is unlikely to be a serious issue at cholesterol contents well below the solubility limit (see, e.g., [18]). The major shortcoming with conventional optical microscopy is that only large domains can be detected. This not only leads to non-detection of phase separation in regions where this is well established by other techniques but also adds to the potential uncertainties in location of phase boundaries that arise from the possibility of light-induced domain formation.

^{2}H NMR cannot detect small domains in regions of fluid–fluid phase separation because averaging takes place by rapid translational exchange. This is not a limitation for gel–fluid phase separation because translational diffusion in the gel phase is very slow. The detection of three-phase coexistence by ^{2}H NMR is an important advance not simply because it confirms thermodynamic expectations for ternary mixtures: it also implies the existence of a three-phase triangle with separate regions of two-phase coexistence bordering its three sides. Location of the three-phase triangle remains, however, one of the greater areas of uncertainty in the published phase diagrams (compare Figs. 5 and 6).

The sides of the three-phase triangle must be almost parallel to the closest tie lines in the adjacent two-phase regions (see Appendix). In the $L_\alpha + L_o$ regions of DOPC/DPPC/cholesterol mixtures, these have a slope of ~0.6 in Fig. 6 and ~0.9 in Fig. 7 (see Table A.1 in the Appendix), i.e., are parallel to lines corresponding to mixtures with cholesterol/DPPC ratios of 0.6 and 0.9, respectively. The slopes of the tie lines in the $L_\alpha + L_o$ regions of DPhyPC/DPPC/cholesterol mixtures are in the higher range with values of 0.8–1.4 (see Fig. 8 and Table A.3). A similar orientation, close to that of mixtures with a cholesterol/DPPC ratio of 1:1, has also been proposed in the SM-containing systems of Figs. 2 and 4 [16,18]. For the $L_\alpha + L_\beta$ two-phase region, one detailed experimental study [44] gives tie lines with a very small slope, i.e., almost parallel to the *x*-axis, in DLPC/DPPC/cholesterol mixtures (see Table A.4 and bottom panel of Fig. 9). Small, but somewhat larger slopes ~0.2 are found for L_α–L_β tie lines in the DOPC/DPPC/cholesterol system (see Table A.1). Tie lines are not yet available in the $L_o + L_\beta$ region of phase coexistence, and this is a principal source of uncertainty. The most conservative approach at the moment is to place them approximately parallel to the *y*-axis, corresponding to the tie line for the binary mixture with cholesterol, i.e., $x = 1$ (see, e.g., [16]).

In spite of the uncertainties and disagreements, ^{2}H NMR (if nothing else) demonstrates that fluid–fluid phase separation, with large domains induced by cholesterol, is possible in membranes of ternary lipid mixtures. Many uncertainties still exist at the cholesterol-containing edges of the phase diagrams summarised here (and even in the middle in Fig. 10) and may be associated with the small size of the domains in these regions. In this connection, it is worth re-emphasizing the finding of $L_\alpha + L_o$ phase coexistence in the binary systems DPPC + cholesterol and PSM + cholesterol, and also that the horizontal phase boundary found in the binary phase diagrams of several lipids (POPC, SEPC, 1-palmitoyl-2-petroselinoylPC, and dimyristoylPC) with cholesterol implies $L_\alpha + L_o$ phase coexistence at temperatures immediately above this three-phase line. In particular, two-component spectra establish L_α–L_o phase coexistence in the binary mixtures DPPC + cholesterol and PSM + cholesterol [38,21],

but so far not for binary mixtures of cholesterol with any unsaturated phosphatidylcholine.

Appendix: Details of tie lines and miscibility critical temperatures in ternary systems

Table A.1. DOPC/DPPC/cholesterol tie lines

Slopes (dy/dx) and coordinates (x,y) of ends of tie lines in DOPC/DPPC/cholesterol mixtures.

T (°C)	L_α		L_o		dy/dx
	x (mol/mol)	y (mol/mol)	x (mol/mol)	y (mol/mol)	
Data from Veatch et al. [29]					
10	0.18	0.23	0.66	0.54	0.64
10	0.16	0.25	0.65	0.54	0.60
10	0.19	0.16	0.83	0.54	0.58
12.5	0.17	0.23	0.68	0.54	0.60
12.5	0.17	0.23	0.61	0.50	0.61
12.5	0.19	0.15	0.85	0.54	0.59
12.5	0.23	0.09	0.91	0.47	0.56
15	0.19	0.25	0.65	0.54	0.63
15	0.19	0.25	0.66	0.52	0.58
15	0.22	0.15	0.72	0.47	0.64
15	0.22	0.14	0.72	0.46	0.64
15	0.25	0.09	0.83	0.43	0.59
17.5	0.22	0.18	0.76	0.52	0.63
17.5	0.26	0.09	0.80	0.41	0.59
17.5	0.31	0.08	0.82	0.35	0.54
20	0.28	0.23	0.69	0.42	0.46
20	0.27	0.22	0.71	0.47	0.57
20	0.28	0.14	0.82	0.41	0.51
20	0.31	0.08	0.84	0.35	0.52
22.5	0.30	0.19	0.76	0.49	0.65
22.5	0.31	0.11	0.80	0.41	0.60
22.5	0.32	0.09	0.84	0.35	0.51
25	0.33	0.12	0.79	0.44	0.69
25	0.37	0.10	0.78	0.35	0.62
10	0.16	0.08	0.87	0.22	0.20
10	0.22	0.05	0.82	0.19	0.23
Data from Davis et al. [38]					
18	0.30	0.16	0.73	0.55	0.91
22	0.33	0.18	0.72	0.55	0.96
28	0.48	0.23	0.68	0.40	0.84

Tie-line connections are not specified in Davis et al. [38]. Values listed here represent "consensus" positions lying close to the reported phase boundaries, allowing for the error bars on end points (not given in Fig. 7).

Table A.2. DPhyPC/DPPC/cholesterol tie lines

Slopes (dy/dx) and coordinates (x,y) of ends of tie lines in DPhyPC/DPPC/cholesterol mixtures. Data from Veatch et al. [39].

T (°C)	L_α		L_o		dy/dx
	x (mol/mol)	y (mol/mol)	x (mol/mol)	y (mol/mol)	
22	0.17	0.16	0.89	0.74	0.80
27	0.25	0.18	0.83	0.71	0.93
32	0.25	0.20	0.83	0.75	0.95
37	0.33	0.22	0.82	0.78	1.15
42	0.39	0.28	0.75	0.78	1.40
45	0.45	0.35	0.75	0.78	1.42

Table A.3. DLPC/DPPC/cholesterol tie lines

Slopes (dy/dx) and coordinates (x,y) of ends of tie lines in DLPC/DPPC/cholesterol mixtures. Data from Chiang et al. [44].

T (°C)	L_α		L_β		dy/dx
	x (mol/mol)	y (mol/mol)	x (mol/mol)	y (mol/mol)	
24	0.30	0	0.85	0	0
24	0.32	0.04	0.85	0.04	0
24	0.36	0.09	0.85	0.10	0.02
24	0.43	0.14	0.85	0.15	0.03
24	0.46	0.15	0.85	0.18	0.07

Table A.4. Miscibility critical temperatures for ternary mixtures

X(low-lipid)	X(high-lipid)	X(chol)	T_{crit} (°C)	Reference
DOPC–d_{62}-DPPC				
0.27	0.53	0.20	30	[29]
0.25	0.50	0.25	20	
0.00	0.75	0.25	48	[38]
0.22	0.50	0.28	39	
0.35	0.35	0.30	30	
0.48	0.20	0.32	12	
DPhyPC–DPPC				
0.25	0.25	0.50	33	[39]
0.33	0.17	0.50	20	

X(low-lipid) is the mole fraction of the lipid component with lower chain-melting temperature (DOPC or DPhyPC) and X(high-lipid) is for the higher-melting lipid (d_{62}-DPPC or DPPC). Critical points are identified either by domain fluctuations seen in fluorescence microscopy [39] or T_2 relaxation enhancement and line broadening of NMR spectra [29,38].

References

[1] C.S. Ejsing, J.L. Sampaio, V. Surendranath, E. Duchoslav, K. Ekroos, R.W. Klemm, K. Simons, A. Shevchenko, Global analysis of the yeast lipidome by quantitative shotgun mass spectrometry, Proc. Natl. Acad. Sci. U. S. A. 106 (2009) 2136–2141.
[2] S. Schreier-Muccillo, D. Marsh, H. Dugas, H. Schneider, I.C.P. Smith, A spin probe study of the influence of cholesterol on motion and orientation of phospholipids in oriented multibilayers and vesicles, Chem. Phys. Lipids 10 (1973) 11–27.
[3] D. Marsh, I.C.P. Smith, An interacting spin label study of the fluidizing and condensing effects of cholesterol on lecithin bilayers, Biochim. Biophys. Acta 298 (1973) 133–144.
[4] D.J. Recktenwald, H.M. McConnell, Phase equilibria in binary mixtures of phosphatidylcholine and cholesterol, Biochemistry 20 (1981) 4505–4510.
[5] J.H. Ipsen, G. Karlstrom, O.G. Mouritsen, H. Wennerstrom, M.J. Zuckermann, Phase equilibria in the phosphatidylcholine-cholesterol system, Biochim. Biophys. Acta 905 (1987) 162–172.
[6] M.R. Vist, J.H. Davis, Phase-equilibria of cholesterol dipalmitoylphosphatidylcholine mixtures—^{2}H nuclear magnetic-resonance and differential scanning calorimetry, Biochemistry 29 (1990) 451–464.
[7] J.L. Thewalt, M. Bloom, Phosphatidylcholine: cholesterol phase diagrams, Biophys. J. 63 (1992) 1176–1181.
[8] K. Simons, E. Ikonen, Functional rafts in cell membranes, Nature 387 (1997) 569–572.
[9] D. Marsh, Handbook of Lipid Bilayers, CRC Press, Boca Raton FL, 1990.
[10] P. Fajer, P.F. Knowles, D. Marsh, Rotational motion of yeast cytochrome oxidase in phosphatidylcholine complexes studied by saturation-transfer electron spin resonance, Biochemistry 28 (1989) 5634–5643.
[11] S. Subramaniam, H.M. McConnell, Critical mixing in monolayer mixtures of phospholipid and cholesterol, J. Phys. Chem. 91 (1987) 1715–1718.
[12] M.D. Collins, S.L. Keller, Tuning lipid mixtures to induce or suppress domain formation across leaflets of unsupported asymmetric bilayers, Proc. Natl. Acad. Sci. USA 105 (2008) 124–128.
[13] M.R. Brzustowicz, V. Cherezov, M. Zerouga, M. Caffrey, W. Stillwell, S.R. Wassall, Controlling membrane cholesterol content. A role for polyunsaturated (docosahexaenoate) phospholipids, Biochemistry 41 (2002) 12509–12519.
[14] M.R. Brzustowicz, V. Cherezov, M. Caffrey, W. Stillwell, S.R. Wassall, Molecular organization of cholesterol in polyunsaturated membranes: microdomain formation, Biophys. J. 82 (2002) 285–298.
[15] S.R. Shaikh, V. Cherezov, M. Caffrey, S.P. Soni, D. LoCascio, W. Stillwell, S.R. Wassall, Molecular organization of cholesterol in unsaturated phosphatidylethanolamines: x-ray diffraction and solid state ^{2}H NMR reveal differences with phosphatidylcholines, J. Am. Chem. Soc. 128 (2006) 5375–5383.
[16] R.F.M. de Almeida, A. Fedorov, M. Prieto, Sphingomyelin/phosphatidylcholine/cholesterol phase diagram: boundaries and composition of lipid rafts, Biophys. J. 85 (2003) 2406–2416.
[17] S.L. Veatch, S.L. Keller, Miscibility phase diagrams of giant vesicles containing sphingomyelin, Phys. Rev. Lett. 94 (2005) 148101.
[18] A. Pokorny, L.E. Yandek, A.I. Elegbede, A. Hinderliter, P.F.F. Almeida, Temperature and composition dependence of the interaction of δ-lysin with ternary mixtures of sphingomyelin/cholesterol/POPC, Biophys. J. 91 (2006) 2184–2197.
[19] D. Marsh, A. Watts, P.F. Knowles, Evidence for phase boundary lipid. Permeability of tempo-choline into dimyristoyl phosphatidylcholine vesicles at the phase transition, Biochemistry 15 (1976) 3570–3578.
[20] C. Reyes Mateo, A. Ulises Acuña, J.-C. Brochon, Liquid-crystalline phases of cholesterol/lipid bilayers as revealed by the fluorescence of *trans*-parinaric acid, Biophys. J. 68 (1995) 978–987.
[21] M.I. Collado, F.M. Goñi, A. Alonso, D. Marsh, Domain formation in sphingomyelin/cholesterol mixed membranes studied by spin-label electron spin resonance spectroscopy, Biochemistry 44 (2005) 4911–4918.
[22] A. Filippov, G. Orädd, G. Lindblom, The effect of cholesterol on the lateral diffusion of phospholipids in oriented bilayers, Biophys. J. 84 (2003) 3079–3086.

[23] R.F.M. de Almeida, J.W. Borst, A. Fedorov, M. Prieto, A.J.W.G. Visser, Complexity of lipid domains and rafts in giant unilamellar vesicles revealed by combining imaging and microscopic and macroscopic time-resolved fluorescence, Biophys. J. 93 (2007) 539–553.
[24] T.T. Mills, S. Tristram-Nagle, F.A. Heberle, N.F. Morales, J. Zhao, J. Wu, G.E.S. Toombes, J.F. Nagle, G.W. Feigenson, Order parameters and areas in fluid-phase oriented lipid membranes using wide angle x-ray scattering, Biophys. J. 95 (2008) 669–681.
[25] J.J. Pan, T.T. Mills, S. Tristram-Nagle, J.F. Nagle, Cholesterol perturbs lipid bilayers nonuniversally, Phys. Rev. Lett. 100 (2008) 198103.
[26] A.G. Ayuyan, F.S. Cohen, Lipid peroxides promote large rafts: effects of excitation of probes in fluorescence microscopy and electrochemical reactions during vesicle formation, Biophys. J. 91 (2006) 2172–2183.
[27] J. Zhao, J. Wu, H. Shao, F. Kong, N. Jain, G. Hunt, G.W. Feigenson, Phase studies of model biomembranes: macroscopic coexistence of $L_\alpha+L_\beta$, with light-induced coexistence of $L_\alpha+L_o$ phases, Biochim. Biophys. Acta 1768 (2007) 2777–2786.
[28] B.D. Ladbrooke, R.M. Williams, D. Chapman, Studies on lecithin–cholesterol–water interactions by differential scanning calorimetry and x-ray diffraction, Biochim. Biophys. Acta 150 (1968) 333–340.
[29] S.L. Veatch, O. Soubias, S.L. Keller, K. Gawrisch, Critical fluctuations in domain-forming lipid mixtures, Proc. Natl. Acad. Sci. USA 104 (2007) 17650–17655.
[30] J.-H. Sachse, M.D. King, D. Marsh, ESR determination of lipid diffusion coefficients at low spin-label concentrations in biological membranes, using exchange broadening, exchange narrowing, and dipole–dipole interactions, J. Magn. Reson. 71 (1987) 385–404.
[31] L.I. Horváth, P.J. Brophy, D. Marsh, Exchange rates at the lipid–protein interface of myelin proteolipid protein studied by spin-label electron spin resonance, Biochemistry 27 (1988) 46–52.
[32] S.L. Veatch, S.L. Keller, Separation of liquid phases in giant vesicles of ternary mixtures of phospholipids and cholesterol, Biophys. J. 85 (2003) 3074–3083.
[33] S.L. Veatch, I.V. Polozov, K. Gawrisch, S.L. Keller, Liquid domains in vesicles investigated by NMR and fluorescence microscopy, Biophys. J. 86 (2004) 2910–2922.
[34] R.F.M. de Almeida, L.M.S. Loura, A. Fedorov, M. Prieto, Lipid rafts have different sizes depending on membrane composition: a time-resolved fluorescence resonance energy transfer study, J. Mol. Biol. 364 (2005) 1109–1120.
[35] M.L. Frazier, J.R. Wright, A. Pokorny, P.F.F. Almeida, Investigation of domain formation in sphingomyelin/cholesterol/POPC mixtures by fluorescence resonance energy transfer and Monte Carlo simulations, Biophys. J. 92 (2007) 2422–2433.
[36] A. Radhakrishnan, H.M. McConnell, Composition fluctuations, chemical exchange, and nuclear relaxation in membranes containing cholesterol, J. Chem. Phys. 126 (2007) 185101-1–185101-11.
[37] F.M. Linseisen, J.L. Thewalt, M. Bloom, T.M. Bayerl, ^{2}H-NMR and DSC study of SEPC-cholesterol mixtures, Chem. Phys. Lipids 65 (1993) 141–149.
[38] J.H. Davis, J.J. Clair, J. Juhasz, Phase equilibria in DOPC/DPPC-d_{62}/cholesterol mixtures, Biophys. J. 96 (2009) 521–539.
[39] S.L. Veatch, K. Gawrisch, S. Keller, Closed-loop miscibility gap and quantitative tie-lines in ternary membranes containing diphytanoyl PC, Biophys. J. 90 (2006) 4428–4436.
[40] M.B. Sankaram, T.E. Thompson, Cholesterol-induced fluid-phase immiscibility in membranes, Proc. Nat. Acad. Sci. USA 88 (1991) 8686–8690.
[41] G.W. Feigenson, Phase boundaries and biological membranes, Ann. Rev. Biophys. Biomol. Struct. (2007) 3663–3677.
[42] G.W. Feigenson, Phase diagrams and lipid domains in multicomponent lipid bilayer mixtures, Biochim. Biophys. Acta 1788 (2009) 47–52.
[43] J.R. Silvius, D. del Giudice, M. Lafleur, Cholesterol at different bilayer concentrations can promote or antagonize lateral segregation of phospholipids of differing acyl chain length, Biochemistry 35 (1996) 15198–15208.
[44] Y.W. Chiang, J. Zhao, J. Wu, Y.H. Shimoyama, J.H. Freed, G.W. Feigenson, New method for determining tie-lines in coexisting membrane phases using spin-label ESR, Biochim. Biophys. Acta 1668 (2005) 99–105.
[45] J. Zhao, J. Wu, F.A. Heberle, T.T. Mills, P. Klawitter, G. Huang, G. Constanza, G.W. Feigenson, Phase studies of model biomembranes: complex behavior of DSPC/DOPC/cholesterol, Biochim. Biophys. Acta 1768 (2007) 2764–2776.
[46] G.W. Feigenson, J.T. Buboltz, Ternary phase diagram of dipalmitoyl-PC/dilauroyl-PC/cholesterol: nanoscopic domain formation driven by cholesterol, Biophys. J. 80 (2001) 2775–2788.